Tidal Deformabilities and Radii of Neutron Stars from the Observation of GW170817

Soumi De, Daniel Finstad, James M. Lattimer, Duncan A. Brown, Edo Berger, and Christopher M. Biwer

Phys. Rev. Lett. **121**, 091102 — Published 29 August 2018

DOI: 10.1103/PhysRevLett.121.091102

Tidal Deformabilities and Radii of Neutron Stars from the Observation of GW170817

Soumi De[1], Daniel Finstad[1], James M. Lattimer[2], Duncan A. Brown[1], Edo Berger[3], and Christopher M. Biwer[1,4]
[1] *Department of Physics, Syracuse University, Syracuse, NY 13244, USA*
[2] *Department of Physics and Astronomy, Stony Brook University, Stony Brook, NY 11794-3800, USA*
[3] *Harvard-Smithsonian Center for Astrophysics, 60 Garden Street, Cambridge, Massachusetts 02139, USA and*
[4] *Applied Computer Science (CCS-7), Los Alamos National Laboratory, Los Alamos, NM, 87545, USA*

We use gravitational-wave observations of the binary neutron star merger GW170817 to explore the tidal deformabilities and radii of neutron stars. We perform Bayesian parameter estimation with the source location and distance informed by electromagnetic observations. We also assume that the two stars have the same equation of state; we demonstrate that for stars with masses comparable to the component masses of GW170817, this is effectively implemented by assuming that the stars' dimensionless tidal deformabilities are determined by the binary's mass ratio q by $\Lambda_1/\Lambda_2 = q^6$. We investigate different choices of prior on the component masses of the neutron stars. We find that the tidal deformability and 90% credible interval is $\tilde{\Lambda} = 222^{+420}_{-138}$ for a uniform component mass prior, $\tilde{\Lambda} = 245^{+453}_{-151}$ for a component mass prior informed by radio observations of Galactic double neutron stars, and $\tilde{\Lambda} = 233^{+448}_{-144}$ for a component mass prior informed by radio pulsars. We find a robust measurement of the common areal radius of the neutron stars across all mass priors of $8.9 \leq \hat{R} \leq 13.2$ km, with a mean value of $\langle \hat{R} \rangle = 10.8$ km. Our results are the first measurement of tidal deformability with a physical constraint on the star's equation of state and place the first lower bounds on the deformability and areal radii of neutron stars using gravitational waves.

PACS numbers: 95.85.Sz, 26.60.Kp, 97.80.-d

Introduction—On August 17, 2017 LIGO and Virgo observed gravitational waves from a binary neutron star coalescence, GW170817 [1]. This observation can be used to explore the equation of state (EOS) of matter at supernuclear densities [2, 3]. This information is encoded as a change in gravitational-wave phase evolution caused by the tidal deformation of the neutron stars [4]. At leading order, the tidal effects are imprinted in the gravitational-wave signal through the binary tidal deformability [4, 5]

$$\tilde{\Lambda} = \frac{16}{13}\frac{(12q+1)\Lambda_1 + (12+q)q^4\Lambda_2}{(1+q)^5}, \qquad (1)$$

where $q = m_2/m_1 \leq 1$ is the binary's mass ratio (c.f. Eq. (34) of Ref. [6]). The deformability of each star is

$$\Lambda_{1,2} = \frac{2}{3}k_2\left(\frac{R_{1,2}c^2}{Gm_{1,2}}\right)^5, \qquad (2)$$

where k_2 is the tidal Love number [4, 5], which depends on the star's mass and the EOS. $R_{1,2}$ and $m_{1,2}$ are the areal radii and masses of the neutron stars, respectively.

In the results of Ref. [1], the priors on $\Lambda_{1,2}$ are taken to be completely uncorrelated, which is equivalent to assuming that each star may have a different EOS. Here, we re-analyze the gravitational-wave data using Bayesian inference [7–9] to measure the tidal deformability, using a correlation between Λ_1 and Λ_2 which follows from the assumption that both stars have the same EOS. We repeat our analysis without the common EOS constraint and calculate the Bayes factor that compares the evidences for these two models. We also fix the sky position and distance from electromagnetic observations [10, 11]. We study the effect of the prior for the component masses by performing analyses with three different priors: the first is uniform between 1 and $2M_\odot$, the second is informed by radio observations of double neutron star binaries, and the third is informed by the masses of isolated pulsars [12].

The common equation of state constraint—To explore imposing a common EOS constraint, we employ a piecewise polytrope scheme [13] to simulate thousands of equations of state. Each EOS obeys causality, connects at low densities to the well-known EOS of neutron star crusts [14], is constrained by experimental and theoretical studies of the symmetry properties of matter near the nuclear saturation density, and satisfies the observational constraint for the maximum mass of a neutron star, $m_{\rm max} \geq 2M_\odot$ [15]. Fig. 1 shows the results of Tolman-Oppenheimer-Volkoff (TOV) integrations [16, 17] to determine Λ as functions of m, R, and the EOS. Each configuration is color-coded according to its radius. In the relevant mass range, Λ generally varies as m^{-6}. For a given mass m, there is an inherent spread of about a factor ten in Λ, which is correlated with R^6. We find that the star's tidal deformability is related to its compactness parameter $\beta = Gm/(Rc^2)$ by the relation $\Lambda \simeq a\beta^{-6}$. We find that $a = 0.0093 \pm 0.0007$ bounds this relation if $1.1M_\odot \leq m \leq 1.6M_\odot$ (note that this is a bound, not a confidence interval). The additional power of β^{-1} in the $\Lambda-\beta$ relation, relative to β^{-5} in Eq. (2), originates because the dimensionless tidal Love number, k_2, varies roughly as β^{-1} for masses $\geq 1M_\odot$, although this is not the case for all masses [17]. For $m \to 0$ we see that $k_2 \to 0$ so that k_2 is proportional to β with a positive power, but since neutron stars with $m < 1\,M_\odot$ are physically unrealistic, that domain is not pertinent in our study.

We observed that, for nearly every specific EOS, the range of stellar radii in the mass range of interest for

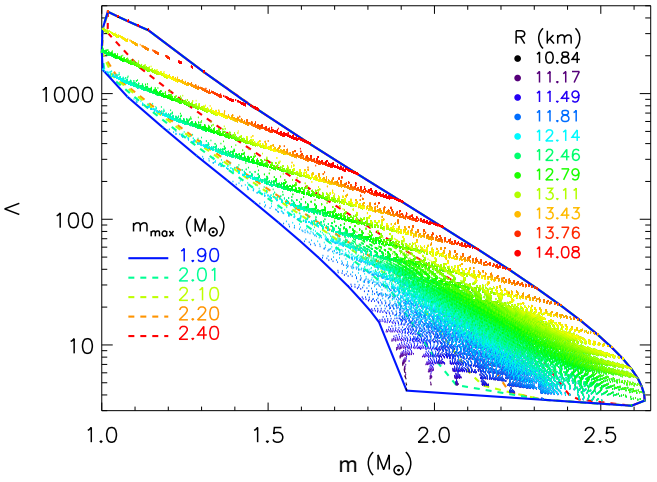

FIG. 1. The tidal deformability Λ as a function of mass for physically realistic polytropes. A TOV integration with each EOS parameter set results in a series of values of $\Lambda(m)$ that are shown as points colored by their radii R. Dashed curves are lower bounds to Λ for a given mass m which vary depending on the assumed lower limit to the neutron star maximum mass, $m_{\rm max}$. All values of $m_{\rm max}$ produce the same upper bound.

GW170817 is typically small. As long as $m_{\rm max} \geq 2M_\odot$, the piecewise polytrope study reveals $\langle \Delta R \rangle = -0.070$ km and $\sqrt{\langle (\Delta R)^2 \rangle} = 0.11$ km, where $\Delta R \equiv R_{1.6} - R_{1.1}$ with $R_{1.1,1.6}$ the radii of stars with $m = 1.1M_\odot$ and $m = 1.6M_\odot$, respectively. Therefore, for masses relevant for GW170817, each EOS assigns a common value of $\hat{R}$ to stellar radii with little sensitivity to the mass. We can combine the relations $\Lambda \simeq a\beta^{-6}$ and $R_1 = R_2$ to find the simple prescription $\Lambda_1 = q^6\Lambda_2$. We impose the common EOS constraint in our analysis using this relation. The exponent of q changes with chirp mass $\mathcal{M}$ and for $\mathcal{M} > 1.5\,M_\odot$ this relation has to be modified. However, this is not relevant for the study of GW170817.

Implications for the neutron star radius—The common EOS constraint allows us to show that the binary tidal deformability $\tilde{\Lambda}$ is essentially a function of the chirp mass $\mathcal{M}$, the common radius $\hat{R}$, and the mass ratio q, but that its dependence on q is very weak. Substituting the expressions $\Lambda \simeq a\beta^{-6}$ and $R = \hat{R}$ into Eq. (1), we find

$$\tilde{\Lambda} = \frac{16a}{13}\left(\frac{\hat{R}c^2}{G\mathcal{M}}\right)^6 f(q). \tag{3}$$

where $f(q)$ is very weakly dependent on q:

$$f(q) = q^{8/5}(12 - 11q + 12q^2)(1+q)^{-26/5}. \tag{4}$$

For example, if we compare a binary with $q = 0.75$ to an equal mass binary, we find $f(0.75)/f(1) = 1.021$. As long as $q \geq 0.6$, valid for $1M_\odot \leq m \leq 1.6M_\odot$ for both stars, we infer from Eq. (3),

$$\tilde{\Lambda} = a'\left(\frac{\hat{R}c^2}{G\mathcal{M}}\right)^6, \tag{5}$$

where $a' = 0.0042 \pm 0.0004$. The supplemental material [56] shows TOV integrations for a range of EOS that validate this relationship. For stars with masses comparable to GW170817, the common radius $\hat{R}$ can be found from the inversion of Eq. (5),

$$\hat{R} \simeq R_{1.4} \simeq (11.2 \pm 0.2)\frac{\mathcal{M}}{M_\odot}\left(\frac{\tilde{\Lambda}}{800}\right)^{1/6} \text{ km}. \tag{6}$$

The quoted errors originate from the uncertainties in a and q, and amount in total to 2%.

Parameter Estimation Methods— We use Bayesian inference to measure the parameters of GW170817 [18]. We calculate the posterior probability density function, $p(\vec{\theta}|\vec{d}(t), H)$, for the set of parameters $\vec{\theta}$ for the gravitational-waveform model, H, given the LIGO Hanford, LIGO Livingston, and Virgo data $\vec{d}(t)$ [19, 20]

$$p(\vec{\theta}|\vec{d}(t), H) = \frac{p(\vec{\theta}|H)p(\vec{d}(t)|\vec{\theta}, H)}{p(\vec{d}(t)|H)}. \tag{7}$$

The prior, $p(\vec{\theta}|H)$, is the set of assumed probability distributions for the waveform parameters. The likelihood $p(\vec{d}(t)|\vec{\theta}, H)$ assumes a Gaussian model for the detector noise [21]. Marginalization of the likelihood to obtain the posterior probabilities is performed using Markov Chain Monte Carlo (MCMC) techniques using the *PyCBC Inference* software [7, 8] and the parallel-tempered *emcee* sampler [9, 22, 23]. We fix the sky location and distance to GW170817 [10, 11] and calculate the posterior probabilities for the remaining source parameters. Following Ref. [1], the waveform model H is the restricted TaylorF2 post-Newtonian aligned-spin model [24–29]. Technical details of our parameter estimation and a comparison to Fig. 5 of Ref [1] are provided as supplemental material [56].

To implement the common EOS constraint we construct the priors on $\Lambda_{1,2}$ according to

$$\Lambda_1 = q^3\Lambda_s, \qquad \Lambda_2 = q^{-3}\Lambda_s, \tag{8}$$

where $\Lambda_s \sim U[0, 5000]$. We discard draws with $\tilde{\Lambda} > 5000$, since these values are beyond the range of all plausible EOS. The resulting prior on $\tilde{\Lambda}$ is uniform between 0 and 5000. We also perform analyses that do not assume the common EOS constraint where we allow completely uncorrelated priors for $\Lambda_{1,2}$. This allows us to compare the evidences between these hypotheses. For the uncorrelated $\Lambda_{1,2}$ analyses, the prior for $\Lambda_1 \sim U[0, 1000]$ and $\Lambda_2 \sim U[0, 5000]$ with these intervals set by the range of plausible equations of state in the mass range of interest, our convention of $m_1 \geq m_2$, and discarding draws with $\tilde{\Lambda} > 5000$.

The choice of mass prior can have an impact on the recovery of the tidal deformability [30]. To investigate this, we carry out our parameter estimation analyses using three different priors on the binary's component masses. We first

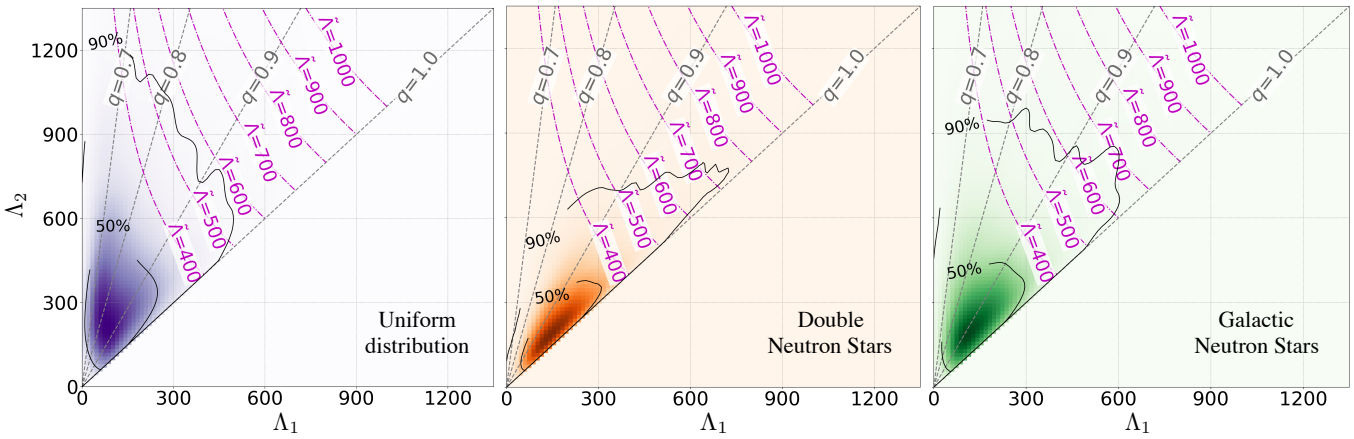

FIG. 2. Posterior probability densities for $\Lambda_{1,2}$ with the common EOS constraint using Uniform (left), Double Neutron Stars (middle), and Galactic Neutron Stars (right) component mass priors. The 50% and 90% credible region contours are shown as solid curves. Overlaid are contours of $\tilde{\Lambda}$ (in magenta) and q (in gray). The values of Λ_1 and Λ_2 forbidden by causality have been excluded from the posteriors.

assume a uniform prior on each star's mass, with $m_{1,2} \sim U[1,2]\,M_\odot$. We then assume a Gaussian prior on the component masses $m_{1,2} \sim N(\mu = 1.33, \sigma = 0.09)\,M_\odot$, which is a fit to masses of neutron stars observed in double neutron star systems [12]. The third prior assumes that the component masses are drawn from a fit to the observed mass distributions of recycled and slow pulsars in the Galaxy with $m_1 \sim N(\mu = 1.54, \sigma = 0.23)\,M_\odot$ and $m_2 \sim N(\mu = 1.49, \sigma = 0.19)\,M_\odot$ [12]. We impose the constraint $m_1 \geq m_2$ which leads to $\Lambda_2 \geq \Lambda_1$. For all our analyses, the prior on the component spins is $\chi_{1,2} \sim U[-0.05, 0.05]$, consistent with the expected spins of field binaries when they enter the LIGO-Virgo sensitive band [31].

Results—We perform parameter estimation for each mass prior with and without the common EOS constraint and calculate the Bayes factor—the ratio of the evidences $p(\vec{d}(t)|H)$—between the common EOS constrained and unconstrained analyses. We find Bayes factors $\mathcal{B}$ of 369, 125, and 612 for the three mass priors, respectively, indicating that the data strongly favors the common EOS constraint in all cases. The full posterior probability densities of the parameters $p(\vec{\theta}|\vec{d}(t), H)$ for the common EOS runs are shown in the supplemental material [56] and are available for download at Ref. [32]. Fig. 2 shows the posterior probability densities for Λ_1 and Λ_2 with 90% and 50% credible region contours. Overlaid are q contours and $\tilde{\Lambda}$ contours obtained from Eq. (1), $\Lambda \simeq a\beta^{-6}$, and $R_1 \simeq R_2 \simeq \hat{R}$ as

$$\Lambda_1(\tilde{\Lambda}, q) = \frac{13}{16}\tilde{\Lambda}\frac{q^2(1+q)^4}{12q^2 - 11q + 12}, \quad \Lambda_2(\tilde{\Lambda}, q) = q^{-6}\Lambda_1 \tag{9}$$

Due to our constraint $\Lambda_2 \geq \Lambda_1$, our credible contours are confined to the region where $q \leq 1$. One can easily demonstrate that $\Lambda_2 \geq \Lambda_1$ is valid unless $(c^2/G)dR/dm > 1$, which is impossible for realistic equations of state. For the entire set of piecewise polytropes satisfying $m_{\rm max} > 2M_\odot$ we considered, $(c^2/G)dR/dm$ never exceeded 0.26. Even if a first order phase transition appeared in stars with masses between m_2 and m_1, it would be necessarily true that $dR/dm < 0$ across the transition. Due to the q dependence of Λ_1, Λ_2, the credible region enclosed by the contours broadens from the double neutron star (most restricted), to the pulsar, to the uniform mass (least restricted) priors. However, the upper bound of the credible region is robust.

We find $\tilde{\Lambda} = 205^{+415}_{-167}$ for the uniform component mass prior, $\tilde{\Lambda} = 234^{+452}_{-180}$ for the prior informed by double neutron star binaries in the Galaxy, and $\tilde{\Lambda} = 218^{+445}_{-173}$ for the prior informed by all Galactic neutron star masses (errors represent 90% credible intervals). Our measurement of $\tilde{\Lambda}$ appears to be robust to the choice of component mass prior, within the (relatively large) statistical errors on its measurement. The Bayes factors comparing the evidence from the three mass priors are of order unity, so we cannot claim any preference between the mass priors.

The 90% credible intervals on $\tilde{\Lambda}$ obtained from the gravitational-wave observations include regions forbidden by causality. Applying a constraint to our posteriors for the causal lower limit of Λ as a function of m [55], we obtain $\tilde{\Lambda} = 222^{+420}_{-138}$ for the uniform component mass prior, $\tilde{\Lambda} = 245^{+453}_{-151}$ for the prior informed by double neutron star binaries in the Galaxy, and $\tilde{\Lambda} = 233^{+448}_{-144}$ for the prior informed by all Galactic neutron star masses (errors represent 90% credible intervals). Using Eq. 6, we map our $\mathcal{M}$ posteriors and $\tilde{\Lambda}$ posteriors (with the causal lower limit applied) to $\hat{R} \simeq R_{1.4}$ posteriors, allowing us to estimate the common radius of the neutron stars for GW170817 for each mass prior. Fig. 3 shows the posterior probability distribution for the binary tidal deformation $\tilde{\Lambda}$ and the common radius $\hat{R}$ of the neutron stars in the binary. Our results

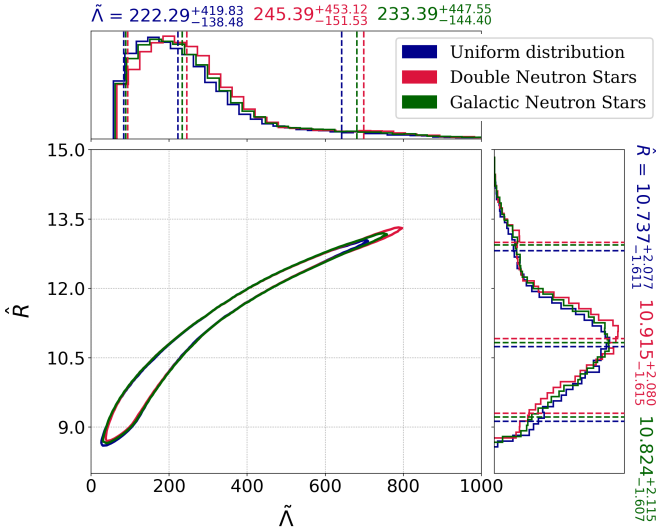

FIG. 3. The 90% credible region of the posterior probability for the common radius $\hat{R}$ and binary tidal deformability $\tilde{\Lambda}$ with the common EOS constraint for the three mass priors. The posteriors for the individual parameters are shown with dotted lines at the 5%, 50% and 95% percentiles. The values of $\tilde{\Lambda}$, and hence $\hat{R}$ forbidden by causality have been excluded from the posteriors.

suggest a radius $\hat{R} = 10.7^{+2.1}_{-1.6} \pm 0.2$ km (90% credible interval, statistical and systematic errors) for the uniform mass prior, $\hat{R} = 10.9^{+2.1}_{-1.6} \pm 0.2$ km for double neutron star mass prior, and $\hat{R} = 10.8^{+2.1}_{-1.6} \pm 0.2$ km for the prior based on all neutron star masses.

For the uniform mass prior, we computed the Bayes factor comparing a model with a prior $\Lambda_s \sim U[0, 5000]$ to a model with a prior $\Lambda_s \sim U[0, 100]$. We find $\log_{10}(\mathcal{B}) \sim 1$, suggesting that the data favors a model that includes measurement of tidal deformability $\tilde{\Lambda} \gtrsim 100$. However, the evidences were calculated using thermodynamic integration of the MCMC chains [9]. We will investigate model selection using e.g. nested sampling [33] in a future work.

Finally, we note the post-Newtonian waveform family used will result in systematic errors in our measurement of the tidal deformability [34, 35]. However, this waveform family allows a direct comparison to the results of Ref. [1]. Accurate modeling of the waveform is challenging, as the errors in numerical simulations are comparable to the size of the matter effects that we are trying to measure [36]. Waveform systematics and comparison of other waveform models (e.g. [37]) will be investigated in a future work.

Discussion—Using Bayesian parameter estimation we have measured the tidal deformability and common radius of the neutron stars in GW170817. Table I summarizes our findings. To compare to Ref. [1], which reports a 90% upper limit on $\tilde{\Lambda} \leq 800$ under the assumption of a uniform prior on $\tilde{\Lambda}$, we integrate the posterior for $\tilde{\Lambda}$ to obtain 90% upper limits on $\tilde{\Lambda}$. For the common EOS analyses these are 485, 521, and 516 for the uniform, double neutron star, and Galactic neutron star component mass priors, respectively.

Mass prior	$\tilde{\Lambda}$	$\hat{R}$ (km)	$\mathcal{B}$	$\tilde{\Lambda}_{90\%}$
Uniform	222^{+420}_{-138}	$10.7^{+2.1}_{-1.6} \pm 0.2$	369	< 485
Double neutron star	245^{+453}_{-151}	$10.9^{+2.1}_{-1.6} \pm 0.2$	125	< 521
Galactic neutron star	233^{+448}_{-144}	$10.8^{+2.1}_{-1.6} \pm 0.2$	612	< 516

TABLE I. Results from parameter estimation analyses using three different mass prior choices with the common EOS constraint, and applying the causal minimum constraint to $\Lambda(m)$. We show 90% credible intervals for $\tilde{\Lambda}$, 90% credible intervals and systematic errors for $\hat{R}$, Bayes factors $\mathcal{B}$ comparing our common EOS to the unconstrained results, and the 90% upper limits on $\tilde{\Lambda}$.

We find that in comparison to the unconstrained analysis, the common EOS assumption significantly reduces the median value and 90% confidence upper bound of $\tilde{\Lambda}$ by about 28% and 19% respectively for all three mass priors. The difference between our common EOS results for the three mass priors is consistent with the physics of the gravitational waveform. At constant $\mathcal{M}$, decreasing q causes the binary to inspiral more quickly [38]. At constant $\mathcal{M}$ and constant q, increasing $\tilde{\Lambda}$ also causes the binary to inspiral more quickly, so there is a mild degeneracy between q and $\tilde{\Lambda}$. The uniform mass prior allows the largest range of mass ratios, so we can fit the data with a larger q and smaller $\tilde{\Lambda}$. The double neutron star mass prior allows the smallest range of mass ratios and so a larger $\tilde{\Lambda}$ is required to fit the data, with the Galactic neutron star mass prior lying between these two cases.

Nevertheless, considering all analyses we performed with different mass prior choices, we find a relatively robust measurement of the common neutron star radius with a mean value $\langle \hat{R} \rangle$ = 10.8 km bounded above by $\hat{R} < 13.2$ km and below by $\hat{R} > 8.9$ km. Nuclear theory and experiment currently predict a somewhat smaller range by 2 km, but with approximately the same centroid as our results [14, 39]. A minimum radius 10.5–11 km is strongly supported by neutron matter theory [40–42], the unitary gas [43], and most nuclear experiments [14, 39, 44]. The only major nuclear experiment that could indicate radii much larger than 13 km is the PREX neutron skin measurement, but this has published error bars much larger than previous analyses based on anti-proton data, charge radii of mirror nuclei, and dipole resonances. Our results are consistent with photospheric radius expansion measurements of X-ray binaries which obtain $R \approx$ 10–12 km [12, 45, 46]. Ref. [47] found from an analysis of 5 neutron stars in quiescent low-mass X-ray binaries a common neutron star radius 9.4 ± 1.2 km, but systematic effects including uncertainties in interstellar absorption and the neutron stars' atmospheric compositions are large. Other analyses have inferred 12 ± 0.7 km [48] and 12.3 ± 1.8 km [49] for the radii of $1.4 M_\odot$ quiescent sources.

We have found that the relation $q^{7.48} < \Lambda_1/\Lambda_2 < q^{5.76}$ in fact completely bounds the uncertainty for the range of $\mathcal{M}$ relevant to GW170817, assuming $m_2 > 1 M_\odot$ [55]

and that no strong first-order phase transitions occur near the nuclear saturation density (i.e., the case in which m_1 is a hybrid star and m_2 is not). Analyses using this prescription instead of the q^6 correlation produce insignificant differences in our results [54]. Since models with the common EOS assumption are highly favored over those without this assumption, our results support the absence of a strong first-order phase transition in this mass range.

In this *letter*, we have shown that for binary neutron star mergers consistent with observed double neutron star systems [50], assuming a common EOS implies that $\Lambda_1/\Lambda_2 \simeq q^6$. We find evidence from GW170817 that favors the common EOS interpretation compared to uncorrelated deformabilities. Although previous studies have suggested that measurement of the tidal deformability is sensitive to the choice of mass prior [30], we find that varying the mass priors does not significantly influence our conclusions suggesting that our results are robust to the choice of mass prior. Our results support the conclusion that we find the first evidence for finite size effects using gravitational-wave observations.

After our *letter* was submitted, the LIGO/Virgo collaborations have placed new constraints on the radii of the neutron stars using GW170817 [51]. The most direct comparison is between our uniform mass prior result ($\hat{R} = 10.7^{+2.1}_{-1.6} \pm 0.2$) and the LIGO/Virgo method that uses equation-of-state-insensitive relations [52, 53] ($R_1 = 10.8^{+2.0}_{-1.7}$ km and $R_2 = 10.7^{+2.1}_{-1.5}$ km). This result validates our approximation $R_1 = R_2$ used to motivate the prescription $\Lambda_1 = q^6\Lambda_2$, and Eqs. 3, 5. Our statistical errors are comparable to the error reported by LIGO/Virgo. Systematic errors from EOS physics of ± 0.2 km are added as conservative bounds to our statistical errors, broadening our measurement error, whereas Ref. [51] marginalized over these errors in the analysis. Ref. [51] also investigates a method of directly measuring the parameters of the EOS which results in smaller measurement errors. Investigation of these differences between our analysis and the latter approach will be pursued in a future paper.

Observations of future binary neutron star mergers will allow further constraints to be placed on the deformability and radius, especially if these binaries have chirp masses similar to GW170817 as radio observations suggest. As more observations improve our knowledge of the neutron star mass distribution, more precise mass–deformability correlations can be used to further constrain the star's radius.

Acknowledgements—We thank Stefan Ballmer, Swetha Bhagwat, Steven Reyes, Andrew Steiner, and Douglas Swesty for helpful discussions. We particularly thank Collin Capano and Alexander Nitz for contributing to the development of PyCBC Inference. This work was supported by NSF awards PHY-1404395 (DAB, CMB), PHY-1707954 (DAB, SD), PHY-1607169 (SD), AST-1559694 (DF), AST-1714498 (EB), and DOE Award DE-FG02-87ER40317 (JML). Computations were supported by Syracuse University and NSF award OAC-1541396. DAB, EB, SD, and JML thank Kavli Institute for Theoretical Physics which is supported by the NSF award PHY-1748958. The gravitational-wave data used in this work was obtained from the LIGO Open Science Center.

[1] B. Abbott *et al.*, Phys. Rev. Lett. **119**, 161101 (2017).
[2] K. S. Thorne, in *Three hundred years of gravitation*, edited by S. W. Hawking and W. Israel (Cambridge University Press, Cambridge, 1987) Chap. 9, pp. 330–458.
[3] J. S. Read *et al.*, Phys. Rev. **D79**, 124033 (2009).
[4] E. E. Flanagan and T. Hinderer, Phys. Rev. **D77**, 021502 (2008).
[5] T. Hinderer, Astrophys. J. **677**, 1216 (2008).
[6] S. E. Gralla, Class. Quant. Grav. **35**, 085002 (2018).
[7] C. M. Biwer, C. D. Capano, S. De, M. Cabero, D. A. Brown, A. H. Nitz, and V. Raymond, (2018), arXiv:1807.10312 [astro-ph.IM].
[8] A. Nitz *et al.*, *PyCBC v1.9.4* (2018).
[9] D. Foreman-Mackey *et al.*, PASP **125**, 306 (2013).
[10] M. Soares-Santos *et al.*, Astrophys. J. **848**, L16 (2017).
[11] M. Cantiello *et al.*, Astrophys. J. **854**, L31 (2018).
[12] F. Özel and P. Freire, Ann. Rev. Astron. Astrophys. **54**, 401 (2016).
[13] J. M. Lattimer and M. Prakash, Phys. Rept. **621**, 127 (2016).
[14] J. M. Lattimer, Ann. Rev. Nucl. Part. Sci. **62**, 485 (2012).
[15] J. Antoniadis *et al.*, Science **340**, 6131 (2013).
[16] J. R. Oppenheimer and G. M. Volkoff, Phys. Rev. **55**, 374 (1939).
[17] S. Postnikov, M. Prakash, and J. M. Lattimer, Phys. Rev. **D82**, 024016 (2010).
[18] N. Christensen and R. Meyer, Phys. Rev. **D64**, 022001 (2001).
[19] M. Vallisneri *et al.*, J. Phys. Conf. Ser. **610**, 012021 (2015).
[20] K. Blackburn *et al.*, *LOSC CLN Data Products for GW170817* (2017).
[21] C. Rover *et al.*, Phys. Rev. **D75**, 062004 (2007).
[22] W. D. Vousden, W. M. Farr, and I. Mandel, Monthly Notices of the Royal Astronomical Society **455**, 1919 (2016).
[23] W. J. Goodman J., Commun. Appl. Math. Comput. Sci. **5**, 65 (2010).
[24] B. S. Sathyaprakash and S. V. Dhurandhar, Phys. Rev. **D44**, 3819 (1991).
[25] A. Buonanno *et al.*, Phys. Rev. **D80**, 084043 (2009).
[26] K. G. Arun *et al.*, Phys. Rev. **D79**, 104023 (2009), [Erratum: Phys. Rev.D84,049901(2011)].
[27] B. Mikoczi, M. Vasuth, and L. A. Gergely, Phys. Rev. **D71**, 124043 (2005).
[28] A. Bohe, S. Marsat, and L. Blanchet, Class. Quant. Grav. **30**, 135009 (2013).
[29] J. Vines, E. E. Flanagan, and T. Hinderer, Phys. Rev. **D83**, 084051 (2011).
[30] M. Agathos *et al.*, Phys. Rev. **D92**, 023012 (2015).
[31] D. A. Brown *et al.*, Phys. Rev. **D86**, 084017 (2012).
[32] S. De *et al.*, *SUGWG GitHub Repository* (2018).
[33] J. Skilling, Bayesian Anal. **1**, 833 (2006).
[34] L. Wade *et al.*, Phys. Rev. **D89**, 103012 (2014).

[35] B. D. Lackey and L. Wade, Phys. Rev. **D91**, 043002 (2015).
[36] K. Barkett *et al.*, Phys. Rev. **D93**, 044064 (2016).
[37] S. Bernuzzi *et al.*, Phys. Rev. Lett. **114**, 161103 (2015).
[38] M. Hannam *et al.*, Astrophys. J. **766**, L14 (2013).
[39] J. M. Lattimer and Y. Lim, Astrophys. J. **771**, 51 (2013).
[40] S. Gandolfi, J. Carlson, and S. Reddy, Phys. Rev. **C85**, 032801 (2012).
[41] J. E. Lynn *et al.*, Phys. Rev. Lett. **116**, 062501 (2016).
[42] C. Drischler, K. Hebeler, and A. Schwenk, Phys. Rev. **C93**, 054314 (2016).
[43] I. Tews, J. M. Lattimer, A. Ohnishi, and E. E. Kolomeitsev, Astrophys. J. **848**, 105 (2017).
[44] I. Tews, T. Krger, K. Hebeler, and A. Schwenk, Phys. Rev. Lett. **110**, 032504 (2013).
[45] A. W. Steiner, J. M. Lattimer, and E. F. Brown, Astrophys. J. **722**, 33 (2010).
[46] N. Degenaar and V. F. Suleimanov, (2018), arXiv:1806.02833 [astro-ph.HE].
[47] S. Guillot and R. E. Rutledge, Astrophys. J. **796**, L3 (2014).
[48] J. M. Lattimer and A. W. Steiner, Astrophys. J. **784**, 123 (2014).
[49] A. W. Shaw *et al.*, (2018), 10.1093/mnras/sty582.
[50] T. M. Tauris *et al.*, Astrophys. J. **846**, 170 (2017).
[51] B. P. Abbott *et al.* (Virgo, LIGO Scientific), (2018), arXiv:1805.11581 [gr-qc].
[52] K. Yagi and N. Yunes, Class. Quant. Grav. **34**, 015006 (2017).
[53] K. Chatziioannou, C.-J. Haster, and A. Zimmerman, Phys. Rev. **D97**, 104036 (2018).
[54] S. De *et al.*, (in preparation) .
[55] T. Zhao and J. M. Lattimer, (In preparation) .
[56] See Supplemental Material for descriptions supporting our implementation of the common radius and causal constraints, technical details of the parameter estimation analysis, full posterior distributions from the common EOS runs, and comparison of results to Ref [1]. The Supplemental Material includes Refs. [57–63] in addition to some of the references included in this letter.
[57] J. Driggers, S. Vitale, A. Lundgren, M. Evans, K. Kawabe, S. Dwyer, K. Izumi, and P. Fritschel, "Offline noise subtraction for Advanced LIGO," (2017), https://dcc.ligo.org/LIGO-P1700260/public.
[58] P. Welch, IEEE Transactions on Audio and Electroacoustics **15**, 70 (1967).
[59] B. Allen, W. G. Anderson, P. R. Brady, D. A. Brown, and J. D. E. Creighton, Phys. Rev. **D85**, 122006 (2012).
[60] T. Damour, A. Nagar, and L. Villain, Phys. Rev. **D85**, 123007 (2012).
[61] T. B. Littenberg and N. J. Cornish, Phys. Rev. **D91**, 084034 (2015).
[62] R. A. Mercer *et al.*, "LIGO Algorithm Library," (2017), https://git.ligo.org/lscsoft/lalsuite.
[63] F. Pérez and B. E. Granger, Computing in Science and Engineering **9**, 21 (2007).